



Evaluation and Restoration of Corrosion-Damaged Post-Tensioned Concrete Structures

Hadif Alsuwaidi ¹, Zaid A. Al-Sadoon ^{1*}, Salah Altoubat ¹, Samer Barakat ¹,
M. Talha Junaid ¹, Mohamed Maalej ¹, Abdulrahman Metawa ¹, Ahed Habib ²

¹ Department of Civil and Environmental Engineering, College of Engineering, University of Sharjah, 27272, Sharjah, United Arab Emirates.

² Research Institute of Sciences and Engineering, University of Sharjah, 27272, Sharjah, United Arab Emirates.

Received 02 September 2024; Revised 19 November 2024; Accepted 27 November 2024; Published 01 December 2024

Abstract

This study addresses the pressing issue of chloride-induced corrosion in post-tensioned (PT) concrete structures, known for their strength and flexibility yet vulnerable to durability issues in extreme climates. The objective is to evaluate corrosion mechanisms in a PT building in the United Arab Emirates and develop a robust restoration strategy. Using a combination of nondestructive and semi-destructive testing methods, this research identifies severe deterioration in critical structural elements, such as steel tendons, PT ducts, and concrete surfaces, largely due to high chloride exposure and aggravated by environmental factors like acid rain and fluctuating temperatures and humidity. The findings reveal serious inadequacies in current maintenance practices, often overlooking long-term corrosion risks in harsh climates. In response, this study proposes a comprehensive repair strategy, including removing damaged materials and applying advanced repair products, protective coatings, and waterproofing measures to enhance the structure's durability. This case study highlights significant concerns regarding structural integrity and provides practical insights into effective maintenance and repair strategies for PT structures. By offering a targeted, sustainable intervention approach, this research contributes to developing PT maintenance protocols, particularly in regions prone to aggressive corrosion, ensuring the longevity and safety of these critical structures.

Keywords: Post-Tensioned Concrete; Corrosion; Chloride Attack; Monitoring; Structural Repair.

1. Introduction

Post-tensioned (PT) concrete structures have substantially enhanced the field of structural engineering by offering improved durability and increased span lengths compared to conventionally reinforced concrete systems. The PT technique involves the application of a pre-compression force to the concrete, counteracting the tensile stresses due to loads applied during service, thus enhancing the structural capacity and serviceability [1, 2]. Despite its advantages, PT structures are susceptible to deterioration over time. The longevity and reliability of PT systems depend on the integrity of their components, most notably the steel tendons that deliver the essential pre-compressive force [3]. The deterioration of PT structures poses a significant challenge, predominantly due to the exposure of steel tendons to environmental attacks such as chloride-induced corrosion [4, 5]. This corrosion is often intensified by materials intended to protect the tendons, namely the grouting material [6-10].

Chloride-induced corrosion is a pervasive issue that significantly affects the durability and structural integrity of post-tensioned concrete structures, which are fundamental to modern infrastructure [11, 12]. The susceptibility of these structures to corrosion, especially when exposed to chloride environments, often leads to premature deterioration, raising

* Corresponding author: zalsadoon@sharjah.ac.ae

 <http://dx.doi.org/10.28991/CEJ-2024-010-12-02>



© 2024 by the authors. Licensee C.E.J, Tehran, Iran. This article is an open access article distributed under the terms and conditions of the Creative Commons Attribution (CC-BY) license (<http://creativecommons.org/licenses/by/4.0/>).

concerns about safety and increasing economic burdens due to repair and maintenance costs [2, 13]. The issue is compounded by the complex interaction between concrete and steel, environmental factors, and preventive measures in place [14, 15]. Extensive research has focused on understanding and mitigating chloride-induced corrosion. Studies like those by Tanaka et al. [11] and Minh et al. [12], have explored the detrimental effects of chloride on the load-carrying capacity of concrete beams and bridges, highlighting the urgency of effective corrosion management strategies. Similarly, [15] have investigated the monitoring techniques for corrosion in steel tendons, providing insights into early detection and management strategies. However, despite advancements in monitoring and repair techniques, as Lee [13] noted, a cohesive review of these strategies and their long-term effectiveness in harsh environments remains scarce.

Within the harsh environment of the United Arab Emirates, characterized by its acid rain and high chloride content in the atmosphere, the vulnerability of PT structures to such aggressive conditions cannot be overlooked [16]. The combination of high temperatures, humidity, and chlorides creates a particularly aggressive environment, accelerating the carbonation process and, consequently, the corrosion of steel tendons [17]. Corrosion phenomena and their mechanisms in PT structures have been extensively studied, revealing a diverse process influenced by factors such as moisture, oxygen, and the availability of corrosive agents [18]. Particularly, pitting corrosion, a localized form of corrosion, poses a severe risk to the structural integrity of PT slabs, as it can lead to sudden and catastrophic tendon failures [19, 20].

The degradation of PT tendons is further compounded by the quality of the grouting material, which can vary significantly, influencing the extent and rate of corrosion [21, 22]. The durability of PT structures is critically compromised by corrosion phenomena, which has garnered significant scholarly attention due to its complex and multifaceted nature [23, 24]. This complex deterioration process consists of a combination of environmental and material factors that precipitate steel corrosion within the concrete, particularly affecting the integrity of PT slabs. The initiation and propagation of corrosion in these structures can be traced to the presence of moisture, oxygen, and corrosive agents, notably chlorides, which are prevalent in coastal areas or regions where deicing salts are commonly employed [25, 26].

The mechanical stresses inherent in prestressed structures can further complicate the corrosion scenario. The high-stress levels in the steel tendons can accelerate the corrosion process at the anode when the conditions at the cathode are conducive, leading to more rapid deterioration and loss of structural integrity [19, 24]. Moreover, environmental factors like temperature fluctuations and humidity levels can significantly influence the rate and extent of corrosion [27]. In warmer climates, increased temperatures can accelerate the chemical reactions that lead to corrosion, while high humidity levels can provide the necessary moisture for these reactions [28]. Corrosion in concrete structures transitions through distinct stages, starting with initiation, where the presence of electrolytes like water contaminated with ions at the rebar surface, PT duct, or strands triggers the onset of corrosion [25].

The propagation phase follows, characterized by the concrete's cracking due to stress from rust layer expansion and a reduction in the steel's effective cross-section, fundamentally undermining the structure's durability [29-31]. Cover depth, reinforcing steel diameter, temperature, moisture, and oxygen availability profoundly influence the corrosion rate [32]. The ingress of chloride ions from groundwater, saline water, rainwater, or construction-used chloride-contaminated water can penetrate the concrete cover or enter through cracks. This compromises the steel's protective passive layer, catalyzing corrosion [15, 32].

In the context of the United Arab Emirates, where PT structures are increasingly common, there is a pressing need for repair strategies tailored to the unique environmental conditions. This includes considerations for the high chloride content and the potential for acid rain, which have been shown to accelerate the deterioration process of PT. The repair strategy must address the immediate structural deficiencies and offer a long-term solution considering ongoing environmental challenges. The preservation and repair of PT structures demand an approach that integrates environmental, material, and design considerations, especially in harsh climates like the United Arab Emirates. Various testing methodologies are employed to comprehensively assess the condition of PT structures and develop effective repair strategies. Nondestructive testing (NDT) techniques such as visual inspection, acoustic emission, and half-cell potential measurements provide valuable information about the structure's condition without causing damage [33]. Semi-destructive methods, including core sampling and chloride content analysis, offer more detailed insights into the material properties and extent of contamination. The selection of appropriate repair techniques is crucial for the long-term performance of rehabilitated PT structures.

Common repair methods include patch repairs, electrochemical chloride extraction, and cathodic protection. However, the effectiveness of these methods can vary depending on the specific environmental conditions and the extent of existing damage [13]. Therefore, a thorough understanding of the local environment and the structure's condition is essential for developing an effective repair strategy [23].

Despite the extensive research on corrosion in PT structures, a significant knowledge gap exists regarding the long-term performance of repair strategies in extreme environmental conditions [34]. In the United Arab Emirates, this region's unique combination of high temperatures, humidity, and chloride exposure presents challenges not fully addressed by existing literature. Furthermore, the interaction between modern grouting materials and the specific environmental conditions remains underexplored, highlighting a critical area for investigation. This study addresses these knowledge gaps by investigating the failure of a PT structure within the United Arab Emirates, aiming to identify root causes and develop a comprehensive repair strategy. By focusing on a case study of a building exhibiting significant

signs of structural corrosion, this research thoroughly examines the complex interplay between environmental factors and material properties leading to PT system deterioration. Through a series of nondestructive and semi-destructive tests, the extent of corrosion damage is assessed, and various repair alternatives are evaluated, ultimately proposing a strategy that balances immediate remediation needs with long-term durability considerations. The adopted research methodology is presented in Figure 1.

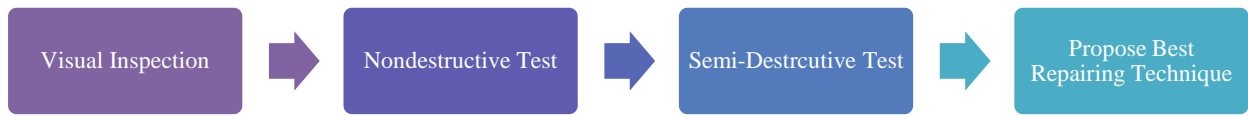


Figure 1. Flowchart showing the adopted research methodology in this study

2. Selected Case Study

The adopted case study herein examines a two-story building due to notable signs of structural deterioration. The building has provided over 24 years of service, comprising halls and offices across its ground and first floors. Recent inspections have revealed concerning signs of delamination and spalling observed on the roof slab soffits. These conditions suggest a probable degradation of the structure's PT tendons, evidenced by the exposure and corrosion of the tendons, alongside cracking. Such deterioration is frequently attributed to the critical issue of reinforcement corrosion. The implications of this case study are significant, highlighting the structural challenges aging structures face in corrosive environments. The findings underscore the importance of practical maintenance and the strategic implementation of repair methodologies to ensure the ongoing safety and functionality of the building users. This study used multiple techniques for nondestructive and semi-destructive tests. For decades, those techniques have shown effectiveness and reliability in assessing concrete structures' durability and deterioration conditions [35].

3. Site Inspection Results

3.1. Visual Inspection

The visual inspection and the acoustic sounding were performed on all accessible surfaces on the ground, first, and roof floors. The visual survey was carried out by closely inspecting all accessible elements and recording all the observed defects. The hammer-sounding survey was carried out by tapping the concrete surfaces with a hammer to detect any sign of hollow-sounding surfaces that generally indicate the presence of concrete delamination. The following section summarizes the main findings from the visual inspection and acoustic-sounding survey. Figure 2 provides a typical defects markup drawing.

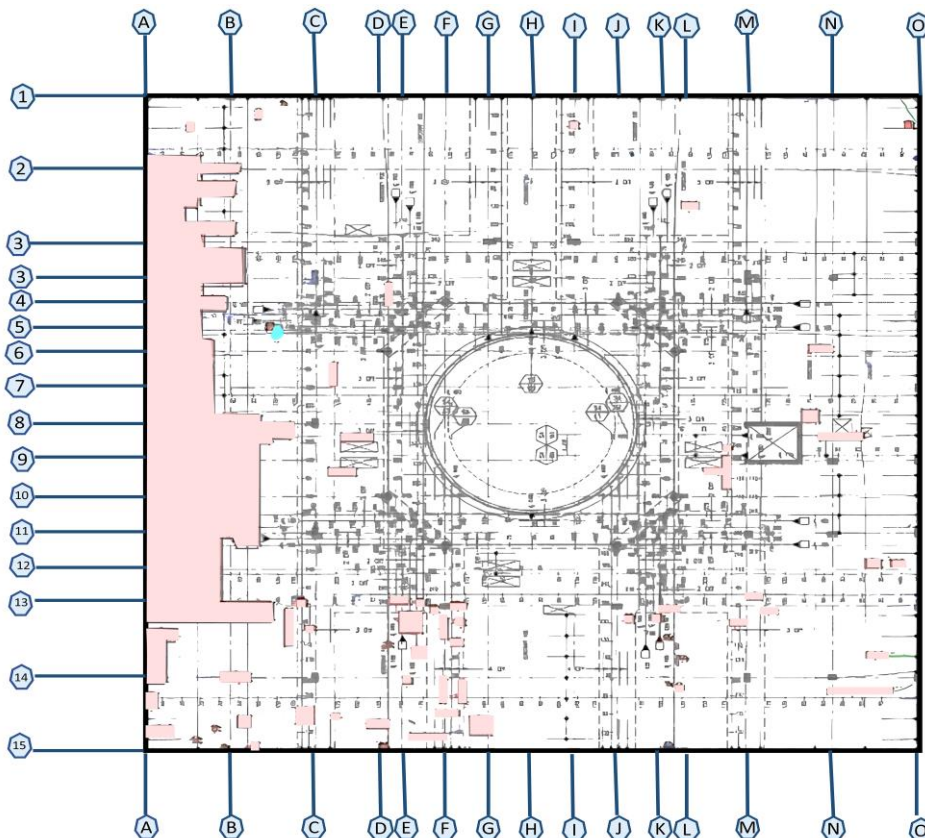


Figure 2. Condition survey of roof slab soffit (Red areas show the affected slab areas)

Based on the visual inspection, it has been noticed that the soffit of the roof slab has spalling, delamination of concrete, exposed corroded PT ducts, and broken PT strands due to corrosion (Figures 3 and 4). During the acoustic survey, hammer tapping in several locations identified Roof slabs as hollow sounds. Dampness and leakage stains were observed in the soffit slab at most of the area (Figure 5). On the other hand, the first-floor slab was in good condition. The locations identified for the testing program were based on the visual inspection findings.



Figure 3. Exposed and corroded broken PT strands at roof slab soffit

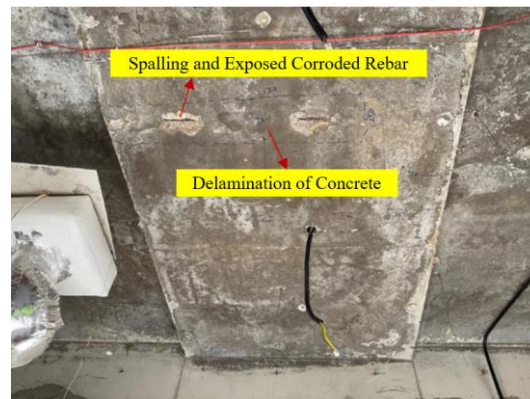


Figure 4. Delamination and spalling of exposed corroded rebar in the roof beam



Figure 5. Leakage stain and dampness in the roof beam

3.2. Concrete Cover and Reinforcement Layout

Woodward concrete cover and reinforcement layout values were measured on-site using ground penetrating radar (GPR). This data was analyzed through Radan 7 [36] software to interpret the position of the steel reinforcement along the survey path and the depth of the steel reported by the radar. A visual representation of the data processed with the software is shown below in Figure 6. The white parabolas indicate the location of steel reinforcement. The longitudinal position of the rebar corresponds to the center of the parabola.

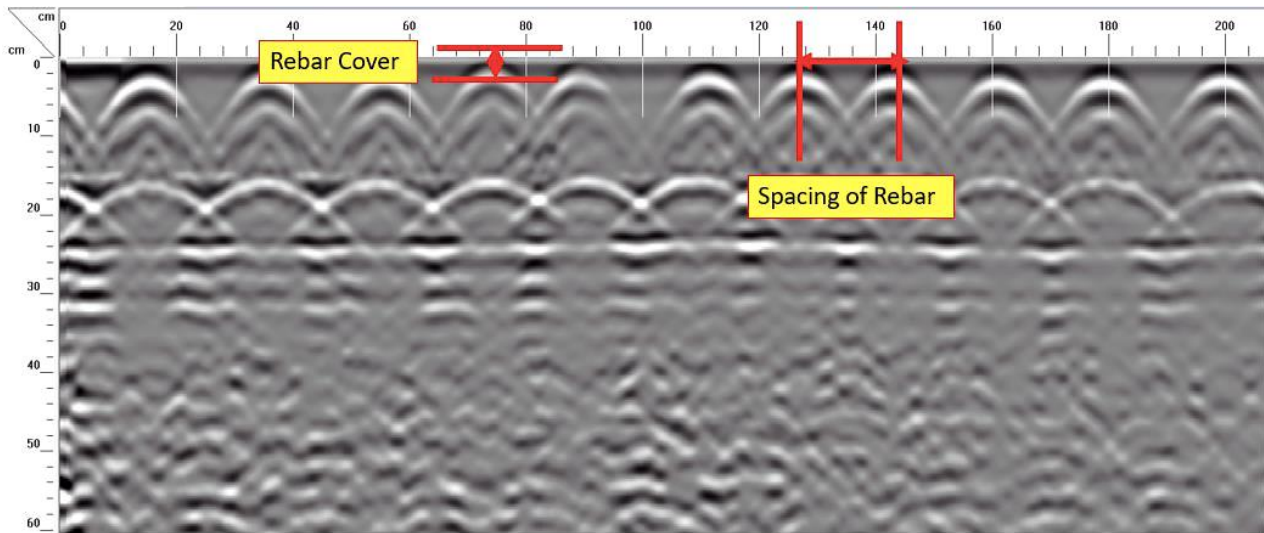


Figure 6. Typical radar data from the cover survey showing the steel reinforcement (FF Beam at Grid A/14-15)

In contrast, the depth of the steel reinforcement corresponds to just below the maxima, where the signal density is greatest (black). The below Table 1 summarizes these results. The concrete cover ranges from 20 to 50 mm for the roof slab. The first-floor slab concrete cover ranges from 50 to 60 mm. Ground and first floor column concrete cover ranges from 25–35 mm to 20–44 mm, respectively. The first-floor beam concrete cover measured 20 mm, and the roof beam concrete cover ranged from 22 to 25 mm.

Table 1. Concrete cover values from radar survey

Ref	Grid Location	Element	Vertical Rebar Spacing (mm)	Horizontal Rebar Spacing (mm)	Concrete Cover (mm)
GPR 1	B-C/12-13	Slab on Grade - Ground Floor	200	200	60
GPR 4	A/2	Ground Floor Wall	180	280	55
GPR 3	A/2	Ground Floor Column	200	5 No. of reinforcement in the range of scan	25
GPR 12	M/3	Ground Floor Column	200	8 No. of reinforcement in the range of scan	35
GPR 7	C/3	First Floor column	100	4 No. of reinforcement in the range of scan	30
GPR 10	O/13	First Floor column	180	5 No. of reinforcement in the range of scan	20
GPR 14	A/2	First Floor column	180	5 No. of reinforcement in the range of scan	44
GPR 2	A/14-15	First Floor Beam - side reinforcement	200 (stirrups)	300 (side reinforcement)	20
GPR 6	C/3-4	Roof Beam	170	--	25
GPR 8	C/14-15	Roof Beam	300	5 No. of reinforcement in the range of scan	25
GPR 15	O/1-2	Roof Beam	170	--	22
GPR 11	N-O/12-13	First Floor Slab	150	--	60
GPR 13	H-I/12-13	First Floor Slab	200	--	50
GPR 5	D-E/6-6'	Roof Slab	200	--	50
GPR 9	C/14-15	Roof Slab	300	No reinforcement observed	32
GPR 16	C-D/14-15	Roof Slab	200	--	25
GPR 17	A-B/5-6	Roof Slab	150	--	20

3.3. Breakout Windows

Breakout window openings were performed on the structure by localized breaking of the concrete cover, thereby exposing rebar to validate the reinforcement condition and concrete cover (Figure 7). The openings revealed that out of nine breakout window locations, one showed corrosion with bar cross-section loss, and two showed rebars with corrosion and surface rust stains. These findings and the half-cell potential (HCP) measurements confirm ongoing corrosion. Table 2 summarizes the findings on the breakout windows.



Figure 7. Typical breakout window at column and roof beam soffit

Table 2. Summary of breakout window findings

Sample ID.	BW Location	Element	Depth of Carbonation (mm)	Measured Rebar Size (mm) X/Y	Window Cover Depth (mm)	Rebar Condition
BW-1	Grid B-C/12-13	Slab on Grade - Ground Floor	0	8/8	70	Good Condition
BW-2	Grid A/2	Ground Floor Column	20	14/14	30	Corroded with section loss
BW-3	Grid A/14-15	First Floor Beam	0	16/12	15	Good Condition
BW-3A	Grid A-B/14-15	First Floor Slab	10	16/16	30	Good Condition
BW-4	Grid C/3-4	Roof Beam	20	12/12	30	Good Condition
BW-5	Grid C/14-15	Roof Slab	0	12/12	25	Mild Surface Rust
BW-5A	Grid C/14-15	Roof Beam	10	12/12	20	Corroded
BW-6	Grid: O/13	First Floor Column	0	8/16	25	Good Condition
BW-6A	Grid: N-O/12-13	First Floor Slab	0	8/12	110	Good Condition

3.4. Carbonation Depth

Carbonation depth was assessed using a phenolphthalein indicator solution that appears pink in contact with alkaline concrete with a pH above 9 and colorless at lower pH levels. The test was carried out by spraying the indicator on freshly exposed concrete surfaces according to BS EN 14630 [37] and RILEM CPC-18 [38]. The carbonation depth of breakout windows/core holes at critical locations only is summarized below in Table 3. The measured carbonation depth observed ranges from 0 to 20 mm. The maximum carbonation depth recorded was observed to be 20 mm in the roof beam soffit slab and ground floor column. However, more than 78% of tested locations were at low risk of corrosion because the reinforcement depth was greater than the carbonation depth.

Table 3. Summary of Carbonation Depth Testing

Sample Id.	BW Location	Element	Window Cover Depth (mm)	Depth of Carbonation (mm)	Risk of Corrosion
BW-2	Grid A/2	Ground Floor Column	30	20	High
BW-3A	Grid A-B/14-15	First Floor Slab	30	10	Moderate
BW-4	Grid C/3-4	Roof Beam	30	20	High
BW-5A	Grid C/14-15	Roof Beam	20	10	High

3.5. Half-Cell Potential Measurements

Half-cell potential measurements were utilized to help determine the risk of corrosion in the areas tested. Before measurements were obtained, the electrical continuity of the steel reinforcing elements (reinforcement bar) was verified. This test evaluates the potential difference between the embedded steel reinforcement and a reference electrode. Since there is continuity in the reinforcement layout of a structure, the potential can be measured from the porous concrete surface when a connection is made with the reinforcement. A connection with the reinforcement is created through an opening, and the continuity of the reinforcement system is verified by checking the connectivity between two distinct openings. A multimeter measures the potential difference between the electrode at the concrete surface and the underlying reinforcement. The measurements are recorded on grids to produce half-cell potential mappings. The readings obtained by performing this test are interpreted to evaluate the probability of active corrosion in the embedded reinforcement. Usually, more negative potentials indicate a higher likelihood of active corrosion. The relationship

between the probability of corrosion and the measured potential depends on the type of reference electrode used for the measurement. A silver/silver-chloride electrode was used to assess the corrosion activity. The ASTM C876 [39] standard provides interpretative guidelines for evaluating corrosion probability for reinforcing steel in concrete as a function of the corrosion potential. Table 4 presents the corrosion probability associated with these electrodes.

Table 4. Half-Cell Test Data

Location	Element/Grid	Maximum steel potential (mV Ag/AgCl)	Minimum steel potential (mV Ag/AgCl)	Absolute Potential Technique (Corrosion Probability)	Potential Difference Technique (Corrosion Probability)
HCP # 1	Slab on Grade; GF @ GF: B/C-12-13	-175	-289	P > 90%	High
HCP # 2	GF-Column; Ground Floor @ GF: A/2	-90	-258	P > 90%	High
HCP # 3	First Floor Slab & Beam @ A/B-14-15	168	-109	10 > P < 90%	High
HCP # 4	Roof Slab Soffit @ C/3-4	171	22	P < 10%	Intermediate
HCP # 5	Roof Slab Soffit & Beam @ C/14-15	-96	-219	10 > P < 90%	High
HCP # 6	First Floor Column @ O/13	-66	-2	P < 10%	Intermediate

3.6. Post-Tension Inspection

The PT system was inspected using nondestructive and semi-destructive methods. The nondestructive evaluation consisted of visual inspection, while the semi-destructive approach involved selective concrete chipping. The examination targeted 12 specific locations on the soffit slabs. Initially, the PT tendons' positions were determined using as-built drawings, with their locations subsequently verified through GPR investigations. The GPR was utilized to identify and mark the PT ducts and any adjacent embedded steel precisely, as well as to measure the depth of the PT ducts from the soffit of the slab. For each selected inspection site, the process began with the chipping away of concrete to document the presence and condition of the grout. In cases where grout was present, it was carefully removed to assess the state of the PT strands underneath. The inspection process included key activities, including capturing photographs of the strands and ducts where access was possible, conducting a visual assessment to identify signs of corrosion both internally and externally, evaluating the corrosion level of the strands against established criteria, and thoroughly documenting the condition of the PT strands and ducts. Table 5 illustrates the condition rating for the PT strands as observed during the inspection. The strands were classified according to the extent of surface rust. Out of the twelve locations inspected, corrosion was detected in the PT ducts at eight sites. Concerning the PT strands, three sites exhibited corrosion. Nevertheless, the grout condition was satisfactory in most of the locations inspected.

Table 5. Sample PT inspection log

Sl. No.	Grid Ref.	Opened by:	Duct Condition	General Strand Condition	Detailed Strand Condition and Notes	Photograph
1	Grid: B-C/5-4 First floor Slab	Drill	Good	Clean	1. Duct Top surface corroded	
		Chip	Poor	Light Rust	2. Mild rust present in strand	
		Spall	Corroded	Medium Rust	3. Grout in good condition	
		Broken	Severe Rust	4. Chloride content below the threshold		
		Non-grouted	Broken Strand			
		Water Inside				
2	Grid: A-B/14-15 Roof Slab Soffit	Drill	Good	Clean	1. Duct Top surface fully corroded	
		Chip	Poor	Light Rust	2. Strand in good condition	
		Spall	Corroded	Medium Rust	3. Grout in good condition	
		Broken	Severe Rust	4. Chloride content below the threshold		
		Non-grouted	Broken Strand			
		Water Inside				
3	Grid: O-N/12-13 Roof Slab Soffit	Drill	Good	Clean	1. Duct Top surface corroded	
		Chip	Poor	Light Rust	2. Strands in good condition	
		Spall	Corroded	Medium Rust	3. Delaminated concrete up to 20 mm	
		Broken	Severe Rust	4. Chloride content below the threshold		
		Non-grouted	Broken Strand			
		Water Inside				

4	Grid: A-B/1-2 Roof Slab Soffit	Drill	Good	Clean	1. Duct were corroded and broken	
		Chip	Poor	Light Rust	2. Strands were broken due to corrosion	
		Spall	Corroded	Medium Rust	3. Delaminated concrete up to 70 mm	
			Broken	Severe Rust	4. Grout were damaged	
			Non-grouted	Broken Strand	5. Grout sample taken 1.5 m away from damaged PT	
			Water Inside		6. Grout sample chloride content below the threshold	

3.7. Concrete Core Sampling

Coring operations were conducted to collect concrete samples for compressive strength testing and chloride/sulfate content analysis at different building locations. A total of thirteen core samples were extracted for compressive strength analysis. For chloride analysis, a total of twenty-one samples were extracted. GPR scans were performed to protect the reinforcements and PT from being damaged.

3.8. Roof Protection System

The roof slab top is covered with several protective layers, including tiles, sand filling, waterproofing, and screed, which prevent complete visual inspection or sounding of the roof slab surface. Waterproofing was removed at one location to check the condition of waterproofing and concrete, while the top layer was covered with tiles. Below, the tiles are covered with 50 mm of sand filling. Underneath, a 4 mm waterproofing sheet was removed. The concrete slab was covered with two layers of screed, 40 mm and 50 mm, respectively. Figure 8 presents the different layers of the waterproofing system found on the roof.

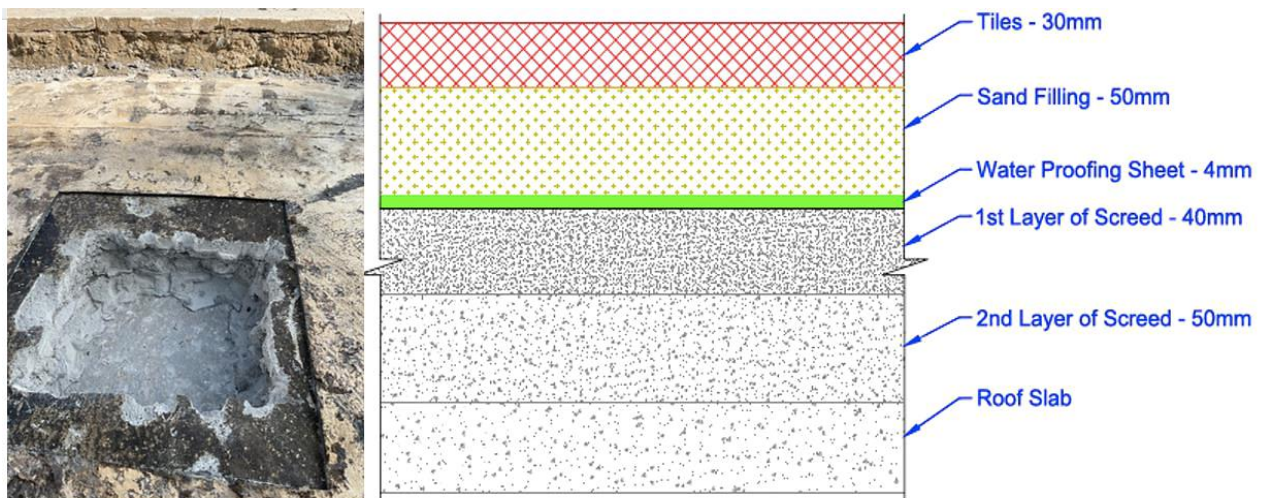


Figure 8. Roof protection system as found at the location with a section showing different layers of protection

4. Laboratory Testing Results

4.1. Compressive Strength

Thirteen concrete core samples were subjected to compressive strength tests as per the guidelines of BS EN 12504:1 2009 [40], which pertains to the testing of concrete within structures, explicitly addressing the extraction, examination, and compression testing of core specimens. The results of these tests are concisely summarized in Figure 9. The range of compressive strengths observed in the samples varied from 19.3 MPa to 40.0 MPa. Notably, the specified design strength for the concrete was 40 MPa cylinder compressive strength (f'_{cu}). Only one of the core samples tested met the designated design strength value. The remaining samples exhibited compressive strengths below the expected threshold. A detailed examination of the testing locations and the concrete cores yielded no evident factors that could account for these lower strength values. Consequently, it is inferred that the concrete compressive strength at most tested locations did not meet the original design specifications.

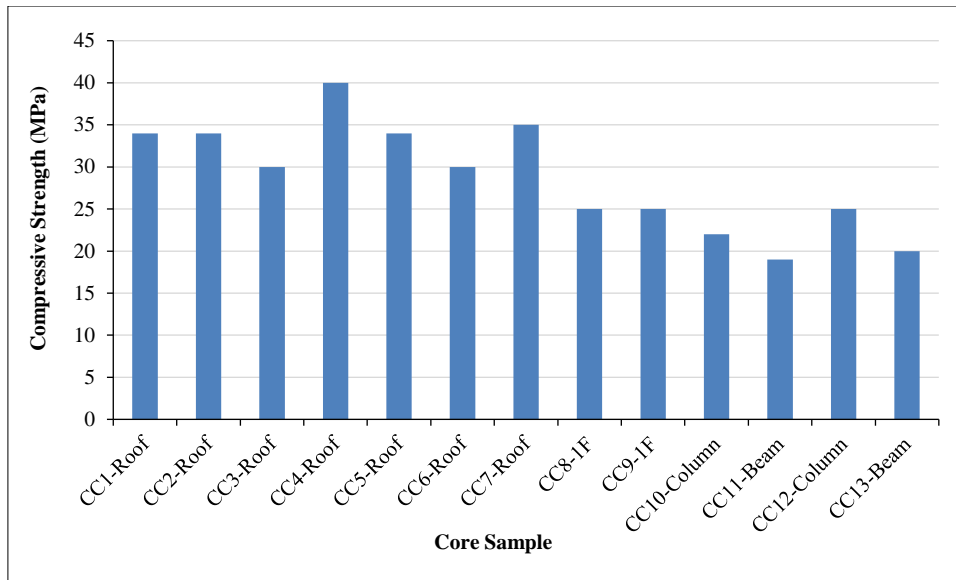


Figure 9. Summary of compressive strength of all elements

4.2. Chloride Ion Contamination Profiles

The chloride content was determined following a procedure adapted from BS 1881-124 [41]. The contamination was evaluated by measuring the total chloride content at various depth increments. The generally accepted threshold is between 0.2% and 0.4% of Chloride per weight of cement. A threshold value of 0.3% of Chloride per sample weight is used for analysis during this study. This can be calculated into a threshold per sample weight, with assumptions as follows: weight of cement (kg/m³) = 380, average unit weight of concrete (kg/m³) = 2256, cement/concrete ratio = 0.168. The threshold per weight of sample = threshold per weight of cement × 0.168 = 0.30 × 0.168 = 0.05%. The data obtained for chloride contamination is presented in Figure 10. The chloride levels for all tested samples were determined to be below the threshold initiating corrosion. However, it should be noted that chloride content in all tested samples can be explained by the chloride-contaminated water used in the concrete mixing, which was reported later on.

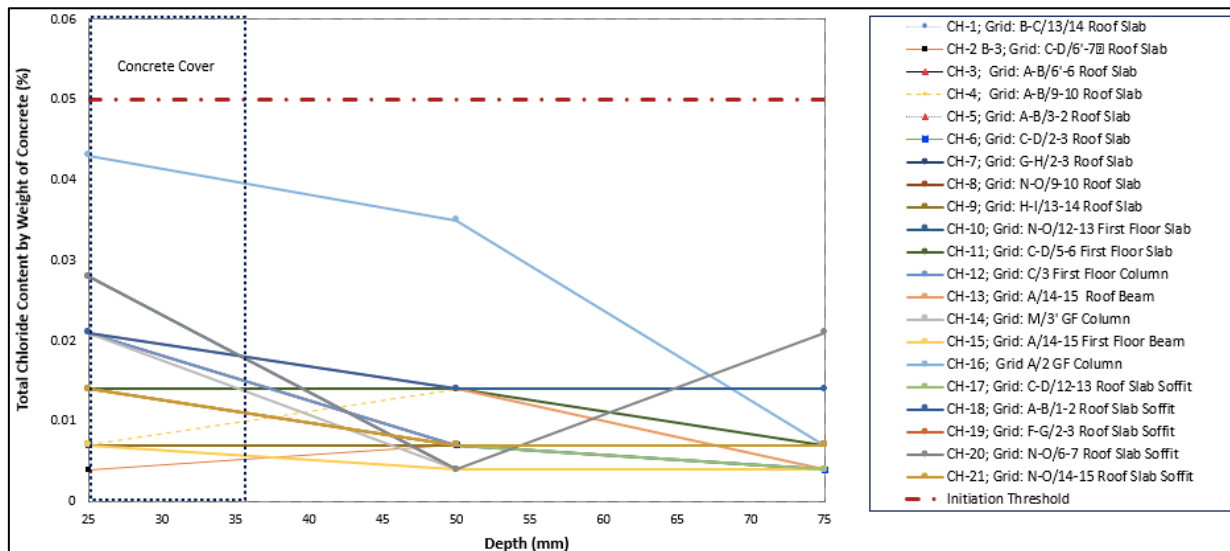


Figure 10. Chloride profile for all elements

4.3. Sulfate Content Analysis

The sulfate content was determined following a procedure adapted from BS 1881-124 [41]. The contamination was evaluated by measuring the total sulfate content at depth increments of 0 to 50 mm. Generally, the maximum allowable total sulfate (SO₃) content of concrete mix from all ingredients, including cement, is limited to 4% by weight of cement. This can be calculated per sample weight; the calculation and assumptions are the weight of cement (kg/m³) = 380, Unit Weight of Concrete (kg/m³) = 2256, and Ratio - Cement: Concrete = 0.168. Therefore, the threshold per Weight of Sample = Threshold per Weight of Cement × 0.168 = 4.00 × 0.168 = 0.67%. The results obtained for sulfate contamination are presented in Table 6. The sulfate content per weight of the sample was between 0.28 and 0.53, below the acceptable threshold of 0.67% by weight of cement.

Table 6. Summary of sulfate contamination

Location	Element	Core ID	From top 0-25 mm	From top 25-50 mm
Grid: B-C/13/14	Roof Slab	CH-1	0.33	0.28
Grid: C-D/6-7	Roof Slab	CH-2	0.38	0.28
Grid: A-B/6-6	Roof Slab	CH-3	0.38	0.33
Grid: A-B/9-10	Roof Slab	CH-4	0.32	0.31
Grid: A-B/3-2	Roof Slab	CH-5	0.35	0.34
Grid: N-O/12-13	First Floor Slab	CH-10	0.53	0.42
Grid: C/3	First Floor Column	CH-12	0.40	0.35
Grid: A/14-15	First Floor Beam	CH-15	0.36	0.35

4.4. PT Grout Sample Chloride Content Analysis

The chloride content was determined following a procedure adapted from BS 1881-124 [41]. PT grout samples were collected after removing the PT duct. The contamination was evaluated by measuring the total chloride content. The threshold per weight of the sample is considered 0.05% by the weight of the concrete. Table 7 presents the total weight of acid-soluble chlorides per sample weight from PT grout samples, expressed in percentage (%). The chloride contents were found to be above the corrosion initiation threshold for 50% of the tested samples.

Table 7. Summary of chloride contamination (%)

Location	Element	Core ID	Chloride Content (% weight of cement)
Grid: B-C/5-4	First Floor Slab	PT-1	0.035
Grid: A-B/14-15	Roof Slab Soffit	PT-2	0.099
Grid: O-N/12-13	Roof Slab Soffit	PT-3	0.092
Grid: A-B/1-2	Roof Slab Soffit	PT-4	0.007
Grid: A-B/3-2	Roof Slab Soffit	PT-5	0.170
Grid: A-B/5-6	Roof Slab Soffit	PT-6	0.035
Grid: D-F/14-15	Roof Slab Soffit	PT-7	0.043
Grid: F-G/14-15	Roof Slab Soffit	PT-8	0.021
Grid: J-K/13-14	Roof Slab Soffit	PT-9	0.064
Grid: A-B/3-3	First Floor Slab	PT-10	0.071
Grid: A-B/14-15	First Floor Slab	PT-11	0.071
Grid: A-B/3-2	First Floor Slab	PT-12	0.028

4.5. Mechanical Test for Steel Reinforcement

Samples of corroded bars were extracted from predetermined locations and subjected to a series of mechanical tests to assess the extent of damage sustained by the steel reinforcement due to corrosion. These tests were designed to evaluate the reinforcement bars' yield strength, ultimate tensile strength, elongation, and other relevant mechanical characteristics. Following the standards outlined in BS 4449:2005 [42], the outcomes of these evaluations are presented in Table 8.

Table 8. Summary of mechanical tests of steel rebars

Location	Element	Sample ID	Bar Diameter (mm)	Eff. Area (mm ²)	Yield Strength (N/mm ²)	Tensile Strength (N/mm ²)	Elongation at max. force (%)	Mass per meter (kg/m)
Grid A-B/14-15	Roof Slab Soffit	ST-1	12	109.8	541	803	6.6	0.862
Grid D-E/6-6	Roof Beam	ST-2	12	108.9	445	717	6.8	0.855
N-O/12-13	First Floor Slab	ST-3	12	108.9	420	678	6.6	0.855

4.6. Rapid Chloride Permeability Test

The rapid chloride permeability test (RCPT), conducted per ASTM C1202 [43], evaluates the permeability of concrete to chloride ions. During the test, a concrete specimen, typically 95 mm in diameter and 50 mm thick and saturated with water, is placed within a test apparatus featuring reservoirs at both ends. One reservoir is filled with a 3% NaCl (sodium chloride) solution, while the opposite reservoir contains a 0.3N NaOH (sodium hydroxide) solution. An

electrical potential of 60 volts DC is applied across the specimen, with the negative terminal linked to the NaCl side and the positive to the NaOH side. This setup encourages the migration of negatively charged ions toward the positive terminal, creating a current through the specimen. The principle underlying this test is that a higher current will be measured if the concrete is more permeable, as this allows greater ion migration.

The current passing through the concrete is recorded for six hours. The total charge passed, measured in Coulombs, is calculated from the area under the current-time curve. The test results in Table 10 indicate the samples' chloride ion penetrability degree. According to the test outcomes, one sample exhibited high chloride ion penetrability, while the remaining showed very high penetrability.

Table 9. Summary of rapid chloride permeability test-RCPT

Location	Element	Core ID	Core Dia./ Length (mm)	Total charge passed in 6 Hrs. (Colbs)	Chloride ion Penetrability
Grid: B-C/13/14	Roof Slab	RCPT-1	94/52	4645	High
Grid: C-D/6-7	Roof Slab	RCPT-2	94/52	Very high; Test stopped at 04:30 hrs. due to over current > 500 mA	
Grid: A-B/6-6	Roof Slab	RCPT-3	94/52	Very high; Test stopped at 01:00 hrs. due to over current > 500 mA	
Grid: G-H/2-3	Roof Slab	RCPT-4	94/52	Very high; Test stopped at 04:15 hrs. due to over current > 500 mA	
Grid: N-O/9-10	Roof Slab	RCPT-5	94/52	Very high; Test stopped at 04:30 hrs. due to over current > 500 mA	
Grid: N-O/12-13	First Floor Slab	RCPT-6	94/52	Very high; Test stopped at 01:05 hrs. due to over current > 500 mA	
Grid: C/3	First Floor Column	RCPT-7	94/52	Very high; Test stopped at 02:40 hrs. due to over current > 500 mA	

Based on the site inspection and laboratory testing results, it can be concluded that corrosion is ongoing in the areas identified as delaminated and sound concrete, mainly due to either loss of alkalinity and/or exposure to moisture. There is also a risk of future corrosion for sound areas if further loss of alkalinity or moisture exposure occurs. Hence, the waterproofing system must be repaired to maintain protection on concrete surfaces and eliminate sources of water ingress.

The following are the main findings from the results section:

- Acoustic surveys using hammer tapping revealed delamination and spalling in the roof slab soffit, notably in areas A-C/1-17, where the damage was most severe.
- Roof soffit slabs exhibited widespread delamination, especially from grid locations A-O/11-17, where spalling and delamination were concentrated.
- Significant moisture penetration and water staining were detected across numerous sections of the roof soffit slab.
- At gridline A-B/5-8, several instances of PT strand exposure and breakage were identified within the roof soffit slab.
- Ground floor columns at gridline A/2 showed concrete delamination and cracking, attributable to rebar corrosion.
- Compressive strength tests indicated values ranging from 19.3 N/mm² to 40.0 N/mm², all below the expected design strength, highlighting widespread structural inadequacy.
- Chloride ion analysis pointed to contamination as the primary cause of corrosion in the PT ducts and strands, with chloride levels exceeding safe thresholds in 50% of PT grout samples, indicating significant corrosion risk.
- The Rapid Chloride Permeability Test demonstrated a high susceptibility to chloride ion penetration in all sampled locations.
- Carbonation depth measurements revealed no carbonation-induced corrosion risk in 80% of locations, though 20% showed conditions conducive to reinforcement corrosion.
- Half-cell potential assessments indicated a high corrosion risk, contrary to LPR readings, suggesting a generally low corrosion probability across most test points.
- Evaluation of PT ducts and strands revealed corrosion in 80% of ducts and 20% of strands, underscoring the prevalent deterioration within the structure.

5. Discussion of Results

The case study presented in this paper highlights critical issues in the durability of PT concrete structures, emphasizing chloride-induced corrosion as the primary cause of deterioration. This failure mechanism, predominantly impacting the steel strands, is a significant concern in structural engineering and concrete technology. The investigation

and subsequent analysis shed light on the complex nature of concrete deterioration, particularly in PT systems, and offer invaluable insights into the interaction of environmental factors and material properties leading to such failures. The corrosion of embedded steel in PT ducts and reinforcement was identified as the primary cause of deterioration. This finding aligns with previous studies, where steel corrosion in concrete is often attributed to chlorides exceeding the threshold for corrosion initiation [44]. However, the study revealed a more complex scenario. While 50% of the PT grout samples showed chloride levels above the corrosion threshold (0.05% by weight of cement), corrosion was observed even in areas where chloride levels were below this threshold. This suggests that factors beyond chloride concentration, such as moisture and oxygen availability, contribute significantly to initiating and propagating corrosion [45].

The damage distribution across the structure was non-uniform, with the roof slab soffit exhibiting the most severe deterioration. Specifically, 80% of inspected areas in the roof slab soffit showed signs of delamination or spalling. Furthermore, 67% of PT ducts examined (8 out of 12) exhibited corrosion, and 25% of PT strands (3 out of 12) showed visible corrosion. In contrast, the first-floor slab was generally in good condition with minimal visible damage, with only 17% of tested areas showing signs of corrosion initiation. Ground floor elements showed localized damage, with 20% of columns displaying signs of concrete delamination. This non-uniform distribution can be attributed to several factors. The roof slab, more exposed to environmental factors, showed significantly more damage than interior elements. Concrete quality also played a role, as compressive strength tests revealed that all samples fell below the design strength of 40 MPa, with values ranging from 19.3 MPa to 40.0 MPa. This lower strength likely contributed to increased permeability and reduced protection against chloride ingress. This is critical as it highlights that repair strategies must address visible structural damage and enhance the concrete's protective properties to mitigate further chloride ingress.

Additionally, the concrete cover ranged from 20 mm to 118 mm, with some areas having insufficient cover (less than 30 mm), particularly in the roof slab. This inadequate cover accelerated the corrosion process in these areas. The study highlights the significant impact of environmental conditions, particularly the role of condensation and water leakage from air conditioning (AC) units in accelerating corrosion. This aligns with findings by Glass et al. [44], who noted that fluctuating wet and dry conditions could significantly accelerate the corrosion process in reinforced concrete. This study extends this understanding to PT structures, where such environmental conditions, coupled with high chloride content in the grouting material, created a conducive environment for corrosion of the PT strands.

The RCPT results further support this conclusion. All tested samples showed either high or very high chloride ion penetrability, with total charge passed ranging from 4645 Coulombs to over 5000 Coulombs (test terminated due to high current). This high permeability explains the widespread chloride contamination, even in seemingly adequate concrete cover areas. The problem of chloride-induced corrosion in the PT strands is particularly concerning. As observed in this study, the presence of chlorides in the PT grout is a critical factor, with 50% of grout samples exceeding the threshold chloride content. This finding aligns with previous research emphasizing the role of grout quality in PT system durability [46]. The corrosive environment around the strands, exacerbated by water ingress, reduces strand thickness and eventual breakage.

The visual survey and test data conclusions resonate with the concept that corrosion is not a surface-level issue but a more profound structural concern. The observation of extensive corrosion in the PT duct and strands, leading to delamination and spalling, are all well-established signs of chloride-induced corrosion. The study's emphasis on treating the causes of corrosion, not just the apparent symptoms, is critical. This approach aligns with modern repair strategies, which advocate for a holistic understanding of the deterioration mechanisms to formulate effective repair and mitigation strategies [47]. The three essential components for corrosion in reinforced concrete, steel, water, and oxygen, as highlighted in our study, are well-established in the literature [48]. However, our case study's emphasis on the interaction of these components in the specific context of PT structures in a harsh environment adds valuable insight to the understanding of concrete durability. Depending on environmental exposure, the observed corrosion rates underscore the need for context-specific evaluation of corrosion risks in PT structures.

6. Rehabilitation and Repair

The evaluation of restoration options was thoroughly investigated, considering the benefits and limitations inherent in each approach. For instance, patch repair, while economically feasible and relatively simple to implement, offers limited durability and may necessitate short-term replacement. On the other hand, the complete reconstruction of deteriorated sections, followed by applying protective coatings, can provide a more robust and enduring solution, addressing both immediate structural concerns and long-term corrosion prevention. It is important to note that a detailed structural assessment must inform the choice of repair method.

When considering PT concrete structure rehabilitation, a comprehensive approach is essential to effectively address visible and dormant deterioration. This approach started with validating as-built drawings through advanced nondestructive methods like GPR. This step was crucial for accurately assessing the structural integrity and planning subsequent repairs [49]. Detecting high chloride content in grout within PT ducts necessitated extensive testing beyond

the visibly affected areas. Such thorough testing was instrumental in representing the extent of contamination and, subsequently, the scope of required remediation efforts.

Regarding the specifics of repair, the main criterion utilized to repair the structure was maintaining its long-term durability. Thus, compromised material was removed due to the complexity of treating spalled and delaminated concrete, and then the reinforcement was thoroughly cleaned. Subsequently, the micro-concrete application was commenced, following ACI standards, which ensure long-term durability [50, 51]. In cases where repairs were not feasible, the repair method shifted to replacement or reconstruction Figure 11. Such a drastic measure must be carefully considered, particularly in areas of severe tendon corrosion. It involved the physical replacement of material, the strategic consideration of PT strand locking, and the integration of new reinforcement in alignment with the results of the conducted structural analysis. The typical steel reinforcement was used to replace the corroded tendons in the damaged slabs to avoid any effect on the existing tendon or reinforcements (Figures 12 and 13).



Figure 11. (a) Concrete cutting to remove significantly deteriorated slab; (b) Removed slab

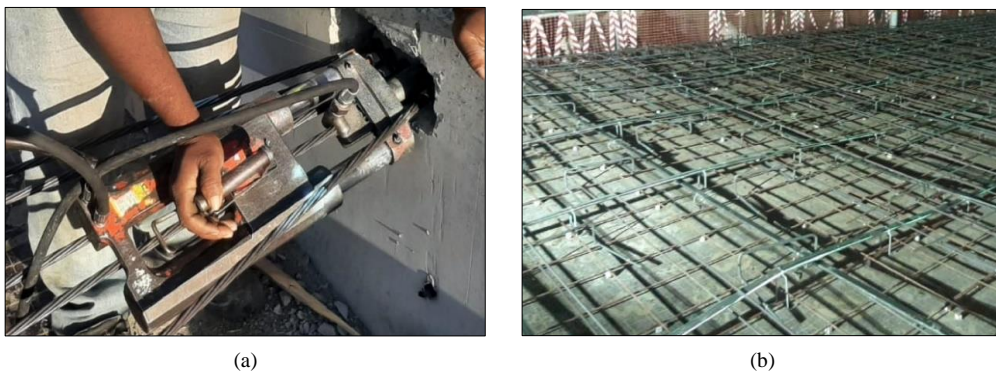


Figure 12. (a) Post-tensioning process; (b) New steel reinforcement

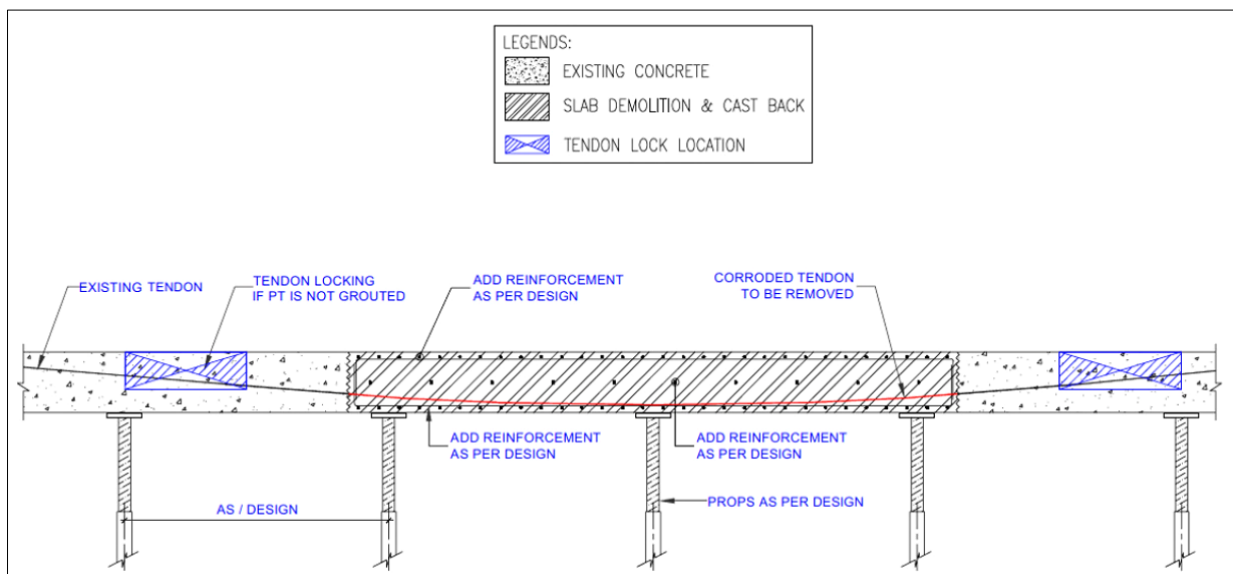


Figure 13. Tendon repair detailing

Furthermore, crack repair in concrete and block walls requires a meticulous approach involving epoxy injections and 'V' groove methods. These are not simple fill-ins but restoration techniques that reestablish the structure's impermeability to moisture, which is a critical factor in stopping the progression of deterioration. Moreover, waterproofing was conducted, which included carefully stripping old, failed systems and the application of advanced waterproofing technologies (Figure 14). Coupled with careful maintenance of roof-level drainage systems, this step repairs existing damage and protects the structure from future water-related deterioration. On the other hand, considering long-term corrosion protection extends beyond immediate repair. These coatings limit oxygen levels at the steel rebar interface, thus significantly reducing the corrosion rate. By inhibiting oxygen penetration and increasing saturation, the coatings reduce the corrosion rate and prevent further infiltration of chlorides or carbonation fronts [9]. Applying these coatings after conventional patch repairs is crucial to protect the reinforcement. Coatings should only be used where corrosion has not yet been initiated, as their effectiveness in mitigating advanced corrosion is limited. In regions where PT grout has shown chloride contamination, maintaining the integrity of the coating system is essential to prevent additional contamination and lessen existing risks.



Figure 14. (a) Old waterproofing removal, (b) New waterproofing

7. Conclusion

This study has thoroughly investigated the deterioration mechanisms in PT concrete structures, focusing on a case study building in the UAE. The research has identified chloride-induced corrosion, facilitated by environmental factors and material properties, as the predominant cause of damage to steel tendons within PT systems. Extensive site inspections, alongside a series of nondestructive and semi-destructive tests, have provided comprehensive data on the extent and nature of the structural damage. The visual and acoustic inspections, chloride content analysis, and mechanical testing of steel reinforcement have all contributed to a detailed understanding of the building's condition. Most of the PT ducts and some strands exhibited signs of corrosion, with grout conditions being satisfactory in most locations. Corrosive processes, as evidenced by the spalling and delamination of concrete and the breakage of PT strands, highlight the urgent need for effective repair strategies. A range of repair alternatives was considered to address the identified issues, with the selected repair strategy aiming to balance immediate remediation needs and long-term durability. The chosen approach involves the comprehensive removal of deteriorated concrete to ensure the long-term durability of the structure and meet the serviceability of newly constructed structures, the application of high-quality repair materials, and the implementation of advanced waterproofing systems to prevent further ingress of moisture and corrosive agents. Additionally, protective coatings were applied to the exposed steel tendons in areas where corrosion has not yet been initiated to inhibit future corrosion risk.

To summarize, the selected repair alternative focuses on restoring the structural integrity of the PT slabs and protecting them against future degradation. It incorporates a series of carefully considered steps, including treating corroded tendons, repairing concrete damage, and enhancing the structure's resistance to environmental attacks. This comprehensive repair approach, informed by the results of the rigorous testing program, is anticipated to not only rehabilitate the existing damage but also extend the service life of the PT structure, ensuring its safety and functionality for future use. This approach can't be compared or copied with similar cases; each case must be well-investigated, and the repair method should be selected based on pre-defined criteria.

8. Declarations

8.1. Author Contributions

Conceptualization, H.A., S.B., Z.A., S.A., M.M., and M.J.; methodology, H.A., Z.A., S.A., S.B., M.M., M.J., and A.H.; validation, H.A., Z.A., S.B., S.A., M.M., M.J., and A.H.; formal analysis, H.A., M.J., Z.A., M.M., S.B., S.A., and A.H.; investigation, H.A., Z.A., M.M., S.A., S.B., M.J., and A.H.; resources, S.A., M.M., and Z.A.; data curation, H.A. and A.H.; writing—original draft preparation, H.A., A.H., and A.M.; writing—review and editing, H.A., Z.A., A.H., M.J., and A.M.; visualization, H.A. and A.H.; supervision, M.M., S.A., and Z.A.; project administration, M.A., S.A., Z.A., and S.B.; funding acquisition, M.A., S.A., and Z.A. All authors have read and agreed to the published version of the manuscript.

8.2. Data Availability Statement

The data presented in this study are available on request from the first author.

8.3. Funding

The authors received no financial support for the research, authorship, and/or publication of this article.

8.4. Conflicts of Interest

The authors declare no conflict of interest.

9. References

- [1] Mangual, J., ElBatanouny, M. K., Ziehl, P., & Matta, F. (2013). Acoustic-emission-based characterization of corrosion damage in cracked concrete with prestressing strand. *ACI Materials Journal*, 110(1), 89–98. doi:10.14359/51684369.
- [2] Menga, A., Kanstad, T., & Cantero, D. (2022). Corrosion induced failures of post-tensioned bridges. Norwegian University of Science and Technology, Trondheim, Norway.
- [3] Kamalakannan, S., Thirunavukkarasu, R., Pillai, R. G., & Santhanam, M. (2018). Factors affecting the performance characteristics of cementitious grouts for post-tensioning applications. *Construction and Building Materials*, 180, 681–691. doi:10.1016/j.conbuildmat.2018.05.236.
- [4] Li, H., Yang, Y., Wang, X., & Tang, H. (2023). Effects of the position and chloride-induced corrosion of strand on bonding behavior between the steel strand and concrete. *Structures*, 58, 105500. doi:10.1016/j.istruc.2023.105500.
- [5] Santarsiero, G., Picciano, V., Masi, A., & Ventura, G. (2024). Retrofit of PRC bridges by external post-tension under different corrosion scenarios. *Bridge Maintenance, Safety, Management, Digitalization and Sustainability*, 571–579, CRC Press, Boca Raton, United States. doi:10.1201/9781003483755-65.
- [6] Emmons, P. H., & Vaysburd, A. M. (1997). Corrosion protection in concrete repair: myth and reality. *Concrete International*, 19(3), 47–56.
- [7] Vennesland, Ø., Raupach, M., & Andrade, C. (2007). Recommendation of Rilem TC 154-EMC: “Electrochemical techniques for measuring corrosion in concrete”—measurements with embedded probes. *Materials and Structures*, 40(8), 745–758. doi:10.1617/s11527-006-9219-4.
- [8] Carsana, M., & Bertolini, L. (2016). Characterization of segregated grout promoting corrosion of posttensioning tendons. *Journal of Materials in Civil Engineering*, 28(6), 04016009. doi:10.1061/(ASCE)MT.1943-5533.0001451.
- [9] Andrade, C. (2023). Role of Oxygen and Humidity in the Reinforcement Corrosion. Proceedings of the 75th RILEM Annual Week 2021. RW 2021, RILEM Bookseries, 40. Springer, Cham, Switzerland. doi:10.1007/978-3-031-21735-7_35.
- [10] Shakouri, M., Abraham, O.F., Vaddey, N.P. (2024). Assessing Passivation and Corrosion of Post-tensioning Strand in Grouts Under Chloride Salt Exposure. *Smart & Sustainable Infrastructure: Building a Greener Tomorrow. ISSSI 2023. RILEM Bookseries*, 48, Springer, Cham, Switzerland. doi:10.1007/978-3-031-53389-1_83.
- [11] Tanaka, Y., Kawano, H., Watanabe, H., & Kimura, T. (2001). Chloride-induced deterioration and its influence on load carrying capacity of post-tensioned concrete bridges. 3rd International Conference on Concrete under Severe Conditions of Environment and Loading (CONSEC'01), 18-20 June, 2001, Vancouver, Canada.
- [12] Minh, H., Mutsuyoshi, H., & Niitani, K. (2007). Influence of grouting condition on crack and load-carrying capacity of post-tensioned concrete beam due to chloride-induced corrosion. *Construction and Building Materials*, 21(7), 1568–1575. doi:10.1016/j.conbuildmat.2005.10.004.
- [13] Lee, S. K. (2022). Corrosion-Induced Durability Issues and Maintenance Strategies for Post-Tensioned Concrete Bridges. No. FHWA-HRT-22-090, Office of Infrastructure Research and Development, Federal Highway Administration, McLean, United States.
- [14] Carsana, M., & Bertolini, L. (2015). Corrosion failure of post-tensioning tendons in alkaline and chloride-free segregated grout: a case study. *Structure and Infrastructure Engineering*, 11(3), 402–411. doi:10.1080/15732479.2014.887736.
- [15] Bertolini, L., Elsener, B., Pedferri, P., Redaelli, E., & Polder, R. B. (2013). Corrosion of steel in concrete: prevention, diagnosis, repair. John Wiley & Sons, Hoboken, United States. doi:10.1002/9783527651696.
- [16] Constantinescu, V., Bogus, G. V., Taran, R. G., & Carcea, I. (2014). New composite materials that reduce the effect of reinforcement corrosion. *Advanced Materials Research*, 837, 265–270. doi:10.4028/www.scientific.net/AMR.837.265.
- [17] Wootton, I. A., Spainhour, L. K., & Yazdani, N. (2003). Corrosion of Steel Reinforcement in Carbon Fiber-Reinforced Polymer Wrapped Concrete Cylinders. *Journal of Composites for Construction*, 7(4), 339–347. doi:10.1061/(asce)1090-0268(2003)7:4(339).

- [18] Al-Mosawe, D., Neves, L., & Owen, J. (2022). Reliability analysis of deteriorated post-tensioned concrete bridges: The case study of Ynys-y-Gwas bridge in UK. *Structures*, 41, 242–259. doi:10.1016/j.istruc.2022.04.094.
- [19] Li, F., Yuan, Y., & Li, C. Q. (2011). Corrosion propagation of prestressing steel strands in concrete subject to chloride attack. *Construction and Building Materials*, 25(10), 3878–3885. doi:10.1016/j.conbuildmat.2011.04.011.
- [20] Wang, L., Hu, Z., Yi, J., Dai, L., Ma, Y., & Zhang, X. (2020). Shear Behavior of Corroded Post-Tensioned Prestressed Concrete Beams with Full/Insufficient Grouting. *KSCE Journal of Civil Engineering*, 24(6), 1881–1892. doi:10.1007/s12205-020-1777-4.
- [21] Joyklad, P., Ali, N., Chaiyasarn, K., Suparp, S., & Hussain, Q. (2022). Time-dependent behavior of full-scale precast post-tensioned (PCPT) girders: Experimental and finite element analysis. *Case Studies in Construction Materials*, 17, e01310. doi:10.1016/j.cscm.2022.e01310.
- [22] Green, W. K., Katen, J. B., & McDonald, D. B. (2021). Long Life Chloride Affected Concrete Structures—Some Corrosion Mechanistic Considerations. *NACE Corrosion*, April, Virtual.
- [23] Permeh, S., & Lau, K. (2023). Assessment of Post-Tensioned Grout Durability by Accelerated Robustness and Corrosion Testing. *Construction Materials*, 3(4), 449–461. doi:10.3390/constrmater3040029.
- [24] Joseline, D., Pillai, R. G., & Neelakantan, L. (2021). Initiation of Stress Corrosion Cracking in Cold-Drawn Prestressing Steel in Hardened Cement Mortar Exposed to Chlorides. *Corrosion*, 77(8), 906–922. doi:10.5006/3730.
- [25] Broomfield, J. P. (2011). Corrosion of Steel in Concrete. *Uhlig's Corrosion Handbook*, 633–647, CRC Press, London, United Kingdom. doi:10.1002/9780470872864.ch49.
- [26] Michałek, J., & Gago, F. (2024). Service Life of Pre-Tensioned Concrete Structures in a Chloride Environment on the Example of an Aluminium Foundry Building. *Materials*, 17(12), 2985. doi:10.3390/ma17122985.
- [27] Liu, X., Zhang, W., Sun, P., & Liu, M. (2022). Time-Dependent Seismic Fragility of Typical Concrete Girder Bridges under Chloride-Induced Corrosion. *Materials*, 15(14), 5020. doi:10.3390/ma15145020.
- [28] Yang, Z.-N., Lu, Z.-H., Li, C.-Q., Liu, X., & Song, X. (2024). Effect of grouting quality on flexural behavior of corroded post-tensioned concrete T-beams. *Case Studies in Construction Materials*, 21, e03766. doi:10.1016/j.cscm.2024.e03766.
- [29] Mehta, P. K. (2006). *Concrete: Microstructure, Properties, and Materials*. McGraw-Hill, New York, United States.
- [30] Yu, Q. Q., Gu, X. L., Zeng, Y. H., & Zhang, W. P. (2022). Flexural behavior of Corrosion-Damaged prestressed concrete beams. *Engineering Structures*, 272, 114985. doi:10.1016/j.engstruct.2022.114985.
- [31] Giriraju, R., Sengupta, A. K., & Pillai, R. G. (2022). Tensile Behaviour of Corroded Strands in Prestressed Concrete Systems. *Journal of The Institution of Engineers (India): Series A*, 103(3), 867–879. doi:10.1007/s40030-022-00656-y.
- [32] Bentur, A. (1997). *Steel Corrosion in Concrete*. CRC Press, London, United Kingdom. doi:10.1201/9781482271898.
- [33] Wang, Y., Pan, Z., Zhao, C., & Zeng, B. (2023). Long-term behavior of prestressed concrete industrial buildings in chloride-based industrial environments. *Journal of Building Engineering*, 76, 107344. doi:10.1016/j.jobbe.2023.107344.
- [34] Lau, K., Permeh, S., & Lasa, I. (2023). Corrosion of prestress and posttension reinforced concrete bridges. *Corrosion of Steel in Concrete Structures*, 81–105. doi:10.1016/B978-0-12-821840-2.00013-4.
- [35] Hoła, J., Bień, J., Sadowski, L., & Schabowicz, K. (2015). Non-destructive and semi-destructive diagnostics of concrete structures in assessment of their durability. *Bulletin of the Polish Academy of Sciences: Technical Sciences*, 63(1), 87–96. doi:10.1515/bpasts-2015-0010.
- [36] Geophysical Survey Systems, Inc. (2017). *RADAN 7*. Geophysical Survey Systems, Inc., Nashua, United States.
- [37] BS EN 14630:2006. (2006). Products and systems for the protection and repair of concrete structures - test methods - determination of carbonation depth in hardened concrete by the phenolphthalein method. British Standard Institute (BSI), London, United Kingdom.
- [38] RILEM CPC-18. (1988). Measurement of Hardened Concrete Carbonation Depth. RILEM 14-20, Descartes, France.
- [39] ASTM C876-22b. (2022). Standard Test Method for Corrosion Potentials of Uncoated Reinforcing Steel in Concrete. ASTM International, Pennsylvania, United States. doi:10.1520/C0876-22B.
- [40] BS EN 12504-1:2009. (2009). Testing concrete in structures. Cored specimens. Taking, examining, and testing in compression. British Standard Institute (BSI), London, United Kingdom.
- [41] BS 1881-124:2015. (2015). Part 124: Methods for analysis of hardened concrete. British Standard Institute (BSI), London, United Kingdom.
- [42] BS 4449:2005+A3:2016. (2016). Steel for the reinforcement of concrete. Weldable reinforcing steel. Bar, coil and decoiled product. British Standard Institute (BSI), London, United Kingdom.

- [43] ASTM C1202-19. (2012). Standard Test Method for Electrical Indication of Concrete's Ability to Resist Chloride Ion Penetration. ASTM International, Pennsylvania, United States. doi:10.1520/C1202-19.
- [44] Glass, G. K., Hassanein, A. M., & Buenfeld, N. R. (2001). Cathodic protection afforded by an intermittent current applied to reinforced concrete. *Corrosion Science*, 43(6), 1111–1131. doi:10.1016/S0010-938X(00)00133-5.
- [45] Hansson, C. M. (1984). Comments on electrochemical measurements of the rate of corrosion of steel in concrete. *Cement and Concrete Research*, 14(4), 574–584. doi:10.1016/0008-8846(84)90135-2.
- [46] Permeah, S., & Lau, K. (2022). Review of Electrochemical Testing to Assess Corrosion of Post-Tensioned Tendons with Segregated Grout. *Construction Materials*, 2(2), 70–84. doi:10.3390/constrmater2020006.
- [47] Tuutti, K. (1982). Corrosion of steel in concrete. Swedish Cement and Concrete Research Institute, Stockholm, Sweden.
- [48] Poursaee, A., & Hansson, C. M. (2009). Potential pitfalls in assessing chloride-induced corrosion of steel in concrete. *Cement and Concrete Research*, 39(5), 391–400. doi:10.1016/j.cemconres.2009.01.015.
- [49] ACI 228.1R-19. (2019). Report on Methods for Estimating In-Place Concrete Strength. American Concrete Institute (ACI), Michigan, United States.
- [50] ACI RAP Bulletin 5. (2003). Surface Repair using Form-and-Pump Techniques. American Concrete Institute (ACI), Michigan, United States.
- [51] ACI RAP Bulletin 6. (2003). Vertical and Overhead Spall Repair by Hand Application. American Concrete Institute (ACI), Michigan, United States.